Journal of Non-Crystalline Solids xxx (2008) xxx–xxx

Contents lists available at ScienceDirect

Journal of Non-Crystalline Solids

journal homepage: www.elsevier.com/locate/jnoncrysol

Polyvinylidene fluoride–hexafluoropropylene (PVdF–HFP)-based composite polymer electrolyte containing $LiPF_3(CF_3CF_2)_3$

V. Aravindan [a], P. Vickraman [a,*], T. Prem Kumar [b]

[a] Department of Physics, Gandhigram Rural University, Gandhigram 624 302, Tamil Nadu, India
[b] Electrochemical Power Systems Division, Central Electrochemical Research Institute, Karaikudi 630 006, Tamil Nadu, India

ARTICLE INFO

Article history:
Received 12 September 2007
Received in revised form 24 December 2007
Available online xxxx

PACS:
61.10.Ed
65.60.+a
61.46.Df

Keywords:
Electrochemical properties
Ceramics
Conductivity
Fast ion conduction
Scanning electron microscopy
Nano-composites
Luminescence
FTIR measurements
Infrared properties
Polymers and organics
Calorimetry

ABSTRACT

This paper describes the preparation and characterization of lithium fluoroalkylphosphate-containing composite polymer electrolyte based on a polyvinylidene fluoride–hexafluoropropylene (PVdF–HFP) matrix. A mixture of ethylene carbonate and diethyl carbonate was used as a plasticizing agent and nanoscopic Al_2O_3 as a filler. The membranes were characterized by ac impedance, SEM, DSC, FTIR and fluorescence. An electrolyte with 2.5 wt% Al_2O_3 exhibited a conductivity of 9.8×10^{-4} S cm^{-1} at ambient temperature. It was found that filler contents above 2.5 wt% rendered the membranes less conducting.

1. Introduction

Classical 'dry' polymer electrolytes based primarily on polymers such as polyethylene oxide (PEO) are solids at room temperature with conductivities typically of the order of 10^{-8} S cm^{-1}. Among approaches that have been adopted to enhance the conductivity and dimensional stability of polymer electrolytes are (i) use of low-volatile liquids of high dielectric constant as plasticizers in the polymer host [1–3], (ii) blending the polymer with another polymer of relatively higher fluidity [4,5], and (iii) incorporation of inert fillers such as γ-$LiAlO_2$ in the polymer film [6,7]. Most studies of polymer as well as organic aprotic liquid electrolytes have been made with $LiPF_6$, the most popular electrolyte salt. $LiPF_6$ possesses several properties desirable for lithium-ion batteries compared to other salts that may be considered in its place [8]. For example, $LiClO_4$ is potentially explosive in contact with organics, $LiBF_4$ interferes with the solid electrolyte interphase (SEI) at the anode (but it has better thermal stability and lower sensitivity towards moisture [9,10], $LiAsF_6$ is toxic, solutions of $LiSO_3CF_3$ have too low conductivities, and $LiN(SO_2CF_3)_2$ and $LiC(SO_2CF_3)_3$ do not effectively passivate the aluminum current collector at the positive electrode, leading to its corrosion [11]. However, $LiPF_6$ is thermally unstable and decomposes to LiF and PF_5 [12,13]. PF_5 hydrolyzes to form HF and PF_3O, which react with both the anode and cathode, deteriorating cell performance [14]. Yet, it is the best compromise available today [8].

Lithium tris(pentafluoroethyl) trifluorophosphate/lithium fluoroalkyl phosphate, $LiPF_3(CF_3CF_2)_3$ (LiFAP) has been proposed as a potential alternative to $LiPF_6$, which is beset with problems of easy hydrolyzability [15–21], as noted above. The premise for its development was that the substitution of one or more fluorine atoms in $LiPF_6$ with perfluorinated alkyl groups would stabilize the P–F bond, rendering the product stable against hydrolysis. In fact, LiFAP exhibits good resistance against hydrolysis. The hydrophobic

* Corresponding author. Tel.: +91 451 2452376; fax: +91 451 2454466.
E-mail addresses: aravind_van@yahoo.com (V. Aravindan), vrsvickraman@yahoo.com (P. Vickraman).

0022-3093/$ - see front matter © 2008 Elsevier B.V. All rights reserved.
doi:10.1016/j.jnoncrysol.2008.03.009

perfluorinated alkyl groups sterically shield the phosphorus center against hydrolysis (see Fig. 1). The new compounds also have conductivities comparable to that of $LiPF_6$. The strong P–F bond also results in an improved thermal stability of the salt. Oesten et al. [17] showed that LiFAP exhibited a far superior stability towards hydrolysis and that electrolytes containing LiFAP exhibited reduced flammability, as a result of the presence in the LiFAP molecule of a combination of flame-retardant moieties, fluorinated derivatives and phosphoric acid esters. Gnanaraj et al. [20,21], who investigated the thermal stability of solutions of $LiPF_6$ and LiFAP in EC–DEC–DMC mixtures using accelerating rate calorimetry, showed that the onset temperature for thermal reactions of LiFAP solutions were higher than 200 °C ($LiPF_6$ solutions: <200 °C) although their self-heating rate was very high. LiFAP is a weakly coordinating bulky anion (anionic size 0.377 nm) because of its large ion contact distance (225 Å^3). It also has a moderate mobility in electrolytes. It has a lower viscosity than $LiPF_6$ and has an ionic conduction comparable to $LiPF_6$ [15]. The FAP anion, which participates in the formation SEI on both anode and cathode, is less prone to contamination by HF and carbonates (solvent reduction products which are major components in the SEI). The lower amount of HF accounts for the lower reactivity of the FAP anion (compared to the PF_6 anion) towards electrodes as well as current collectors. Thus, detrimental electrode-solution reactions that favor the development of surface films are prevented. In the present study, we have prepared nano-composite polymer electrolytes (CPE) with a skeleton of polyvinylidene fluoride–hexafluoropropylene (PVdF–HFP), ethylene carbonate (EC) and diethyl carbonate (DEC) as plasticizing agents, and nanoscopic Al_2O_3 as filler.

2. Experimental

2.1. Materials and methods

LiFAP was received gratis from Merck KGaA, Germany, as a complex with dimethoxyether (DME) [$LiPF_3(CF_3CF_2)_3 \cdot 3DME$]. Ethylene carbonate (EC), diethyl carbonate (DEC), nanoscopic Al_2O_3 (5.8 nm; 155 m^2/g) and tetrahydrofuran (THF) were high purity chemicals from Sigma-Aldrich. Polyvinylidene fluoride–hexafluoropropylene (PVdF–HFP) with 12 mol% of HFP was obtained from Solvay Solexis, Italy. An appropriate amount of the salt was dissolved in a 1:1 (by weight) solvent mixture of EC and DEC. The solvent mixture has a higher boiling point than DME. The LiFAP–DME complex in the EC/DEC solvent was heated at 90 °C in order to completely remove DME (confirmation by FTIR). Polymer electrolyte membranes were prepared according to the compositions shown in Table 1 by a solution casting technique.

2.2. Instrumentation

Ionic conductivities of the membranes were measured by ac impedance spectroscopy in the frequency range 5 MHz–1 Hz by using a Solartron 1260 Impedance/Gain Phase Analyzer coupled with a Solartron Electrochemical Interface. The conductivity cell consisted of two circular stainless steel blocking electrodes (SS/CPE/SS) of 1 cm^2 cross-sectional area. The FTIR spectrum was recorded between 4000 cm^{-1} and 400 cm^{-1} in the transmittance mode using a Jasco 460 Plus IR spectrophotometer with a resolution of 4 cm^{-1}. Morphological features of the membranes were examined by using a Hitachi Model S-3000H scanning electron microscope. Differential scanning calorimetric traces were recorded using a Perkin Elmer Pyris 6 instrument. The thermal events were recorded in nitrogen between 40 °C and 240 °C at a heating rate of 10 °C/min. A Perkin Elmer LS 55 luminescence spectrometer was used for fluorescence depolarization measurements. The sample holder was placed at an angle of 60° against the excitation length. The emission and excitation wavelengths were fixed at 360 nm and 280 nm, respectively.

Table 1
Composition of polymer electrolytes*

Sample	PVdF–HFP	Plasticizer		LiFAP	Al_2O_3
		EC	DEC		
S1	30	32.50	32.50	5	00.0
S2	30	31.25	31.25	5	02.5
S3	30	30.00	30.00	5	05.0
S4	30	28.75	28.75	5	07.5
S5	30	27.50	27.50	5	10.0

* The combinations are in weight ratios.

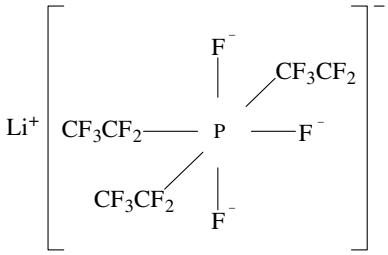

Fig. 1. Structure of LiFAP.

3. Results and discussion

3.1. Ac impedance

A typical impedance spectrum recorded with the CPE (PVdF–HFP 30% + EC:DEC 62.5% + LiFAP 5% + Al_2O_3 2.5%) is given in Fig. 2a while the variation of ionic conductivity with plasticizer (EC + DEC) content at various loadings of the filler is shown in Fig. 2b. It can be seen that conductivity of the filler-free membrane is 0.51 m S cm^{-1}. The value of conductivity increases up to a filler content of 2.5 wt%, at which concentration reaches a maximum value of 0.98 mS.cm^{-1}. A further increase in the filler content leads to a fall in conductivity. The drop in conductivity with increasing filler content may be attributed to an aggregation of nanoscopic Al_2O_3, strongly impeding polymer chain movement. These results are in agreement with our findings with polymer membranes containing LiBOB [22]. However, Nan et al. [23] in their studies with CPEs comprising PEO + EC/PC + $LiClO_4$ + SiO_2 showed that a conductivity maximum occurred at an SiO_2 level of 15 wt%. Although the nature of the filler material has an important influence on the conductivity behavior, other factors may also come into play. For example, the bulky and weakly coordinating FAP anion may be expected to act as a plasticizer, lowering the amount of filler material required to obtain reasonable conductivity values. Moreover, the strong polarizing effect of the smaller ClO_4^- can also influence charge transport. Fig. 3 presents plots of conductivity versus $1/T$ for the CPEs. The curvature in the plot shows that ionic conduction in the polymer electrolyte obeys the VTF (Vogel–Tamman–Fulcher) relation, which describes the transport properties in a viscous polymer matrix [24].

It can be seen that a CPE containing 2.5 wt% filler exhibits a conductivity of 2.12 m S cm^{-1} at 70 °C. An increase in temperature leads to an increase in conductivity. This is only expected because as the temperature increases the polymer expands to produce free volume, which leads to enhanced ionic mobility and polymer segmental mobility. The enhancement of ionic conductivity by the filler particles can be explained by the fact that the particles inhibit recrystallization kinetics, helping to retain the amorphous phase down to

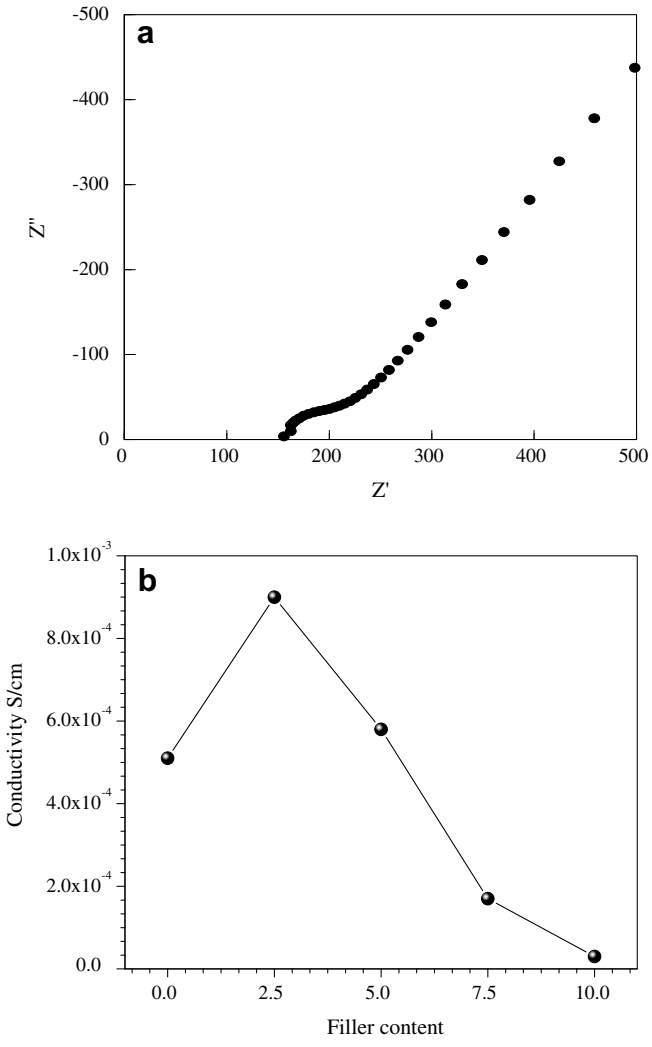

Fig. 2. (a) A typical impedance spectrum of the CPE (2.5 wt% Al_2O_3). (b) Variation of ionic conductivity with filler content.

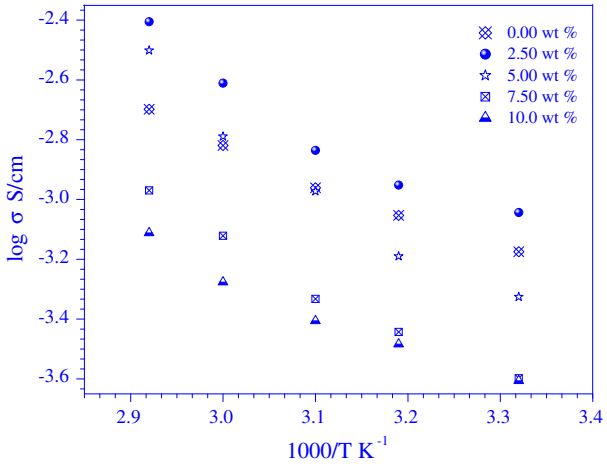

Fig. 3. Temperature dependence of the ionic conductivity of a composite polymer electrolyte.

relatively low temperatures. At the same tine, plasticizers contribute to conductivity enhancement by opening up narrow rivulets of plasticizer-rich phases for greater ionic transport, generating large free volumes of relatively enhanced conducting phases [25].

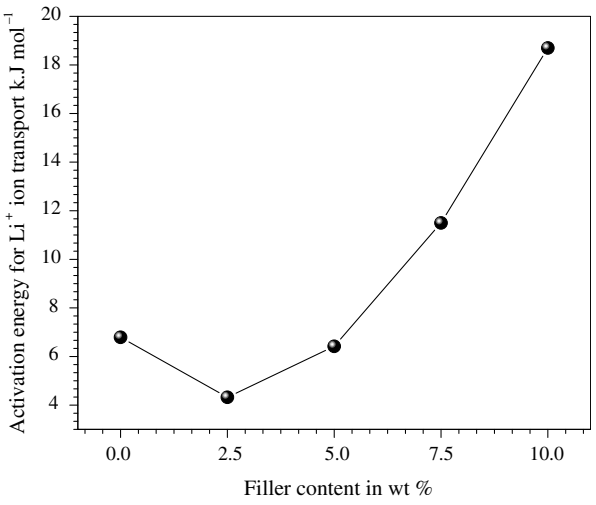

Fig. 4. Activation energy at different filler concentrations.

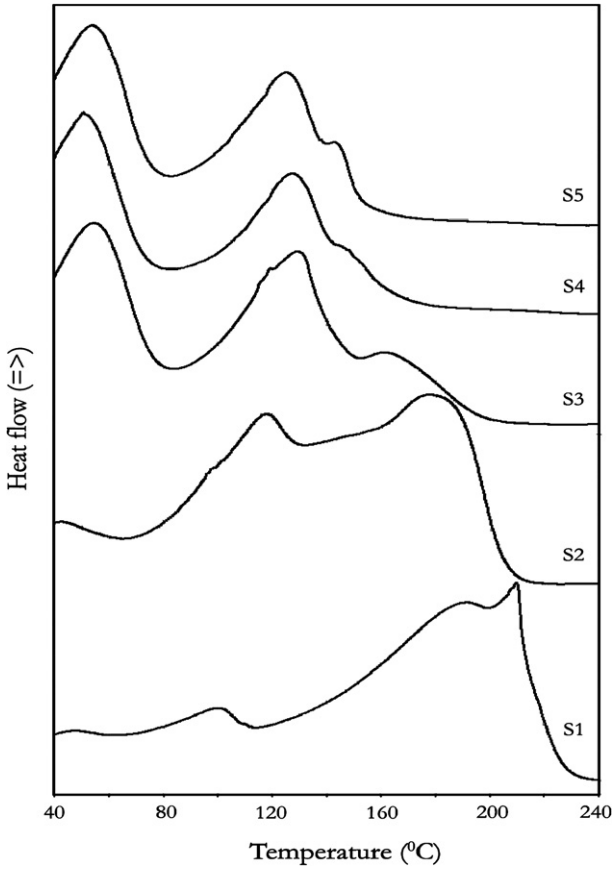

Fig. 5. Differential scanning calorimetric profiles of CPEs containing 0.0 (S1), 2.5 (S2), 5.0 (S3), 7.5 (S5), and 5.0 wt% (S5) filler.

3.2. Activation energy for Li^+ ion transport

Fig. 3 depicts the dependence of ionic conductivity on temperature in the range 27–70 °C for the polymer electrolyte. The activation energy for ion transport, E_a, can be obtained by using the Vogel–Tamman–Fulcher model:

$$\sigma = \sigma_0 T^{-1/2} \exp\left(\frac{-E_a}{T - T_0}\right), \quad (1)$$

where σ is ionic conductivity, σ_0 is pre-exponential factor and T_0 is glass transition temperature. Fig. 4 shows the relationship between

the amount of filler in the membrane and the activation energy for ionic transport. Our results suggest that the activation energy for ionic transport decreases as the filler concentration is increased for filler levels up to 10 wt%. However, at higher filler levels, the activation energy increases. The activation energy drops to 4.32 kJ mol^{-1} when the mass fraction of the filler equals 2.5%.

3.3. Differential scanning calorimetry

DSC profiles of PVdF–HFP films filled with different contents of filler particles were measured to investigate the change in polymer crystal properties due to filler addition (Fig. 5). As the Al_2O_3 content increases, the T_m of cast film suffers an irregular pattern of decrease and increase. This behavior is related to the crystal phases of VdF during heating and melting [26]. The films exhibit some melting peaks corresponding to VdF crystals (e.g., α- and γ-phases) in the range of 120–190 °C, corresponding to the melting of the α-phase (big spherulite) crystals. The peak around 100 °C in the filler-free electrolyte may be due to boiling of DEC. By adding 2.5 wt% of nanoscopic Al_2O_3, the T_m shifted to a lower temperature, which leads to a decrease in crystallinity. Furthermore, increasing the filler content up to 10 wt%, a broad T_m starts at around to 128 °C (the onset temperature of T_m starts at around 85 °C), which includes the boiling point of DEC and the T_m of VdF crystals α-phase crystals. At the same time a small kink around 165 °C may be due to the existence of the same α-phase crystals. The slight shift of T_m or the small change of crystal phase brought about by the addition of Al_2O_3 can be understood in terms of a localized influence on the polymer chain conformation resulting from some dipole orientation properties of Al_2O_3. The endothermic event at around 60 °C may be due to the nano-crystalline phase change of Al_2O_3 [27].

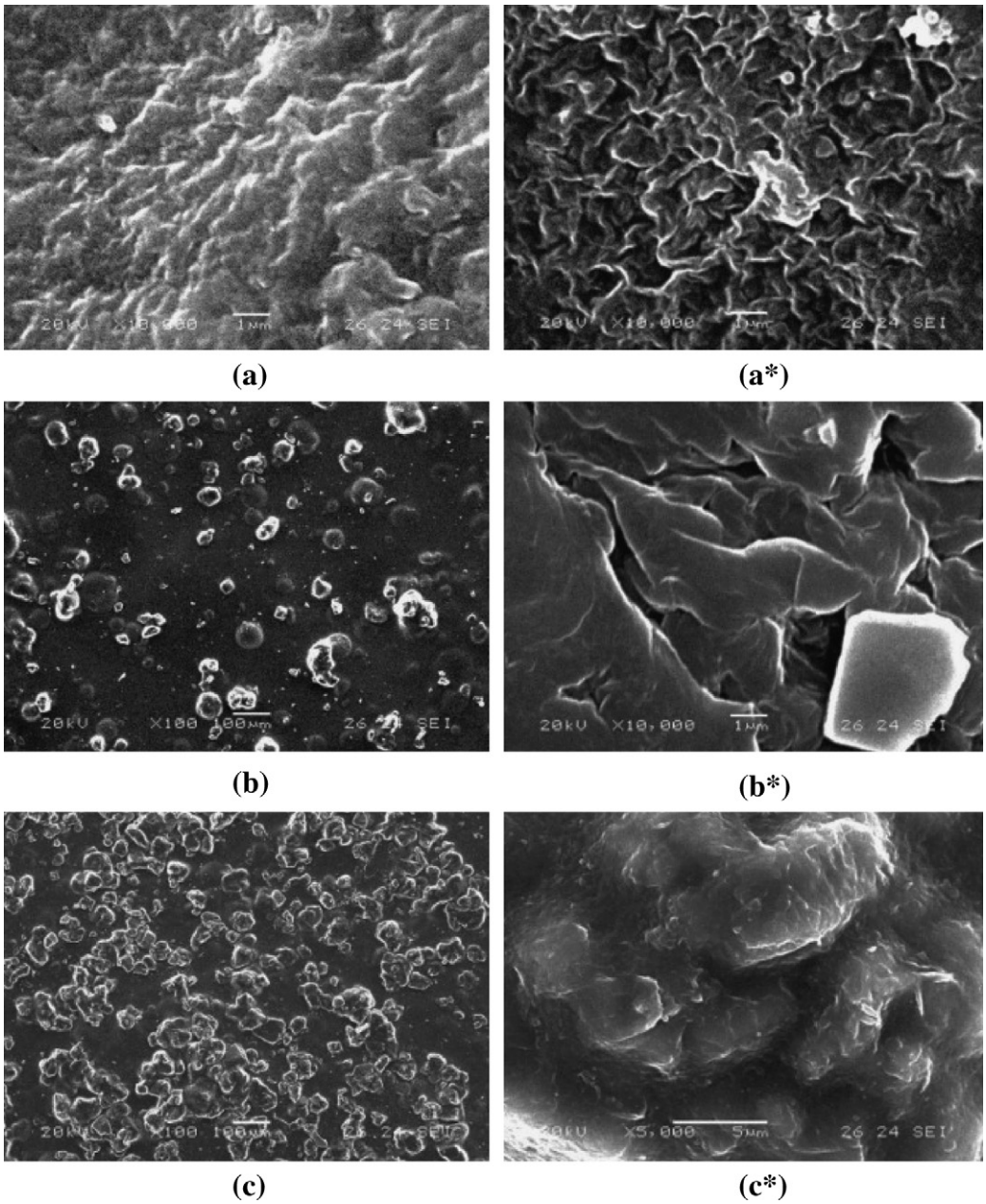

Fig. 6. Scanning electron images of CPEs with different filler ratios (wt%) (a) 0.0, (b) 2.5, and (c) 5.0.

3.4. Morphological studies

The opacity of the film is increased by increasing the filler content. Fig. 6 shows the SEM images of CPEs with 0 wt% (Fig. 6a and a*), 2.5 wt% (Fig. 6b and b*), and 5.0 wt% (Fig. 6c and c*). The filler-free membrane shows a highly porous structure. The presence of pores may be due to accumulation of the plasticizer between the interconnected networks of the polymer matrix. Addition of a small amount, say, 2.5 wt% of the filler, leads to an improvement in the morphology of the membrane. Upon increasing the filler content to 5 wt%, the filler particles get unevenly dispersed in the matrix, resulting in an aggregation of the particles. The clustered particles impede ionic conduction as is evident from Fig. 2.

Generally, conductivity in conventional polymer electrolytes is achieved through continuous pathways of absorbed liquid electrolyte within interconnected pores of membranes. Thus, a highly developed porous structure is a prerequisite for a good ionically conducting separator [28]. It is, therefore, clear that in such a structure, ionic conductivity of the electrolyte is a major determinant [29]. Thus, the conductivity of an electrolyte-laden membrane is influenced by membranes porosity, tortuosity of the pores, the conductivity of the liquid electrolyte, the thickness of the membrane, and the extent of wetting of the membrane by the electrolyte. In the case of composite electrolytes, the porous structure of the membranes tend towards a non-porous one when filler concentrations exceed 2.5 wt%, as is evident from a drop in conductivity above this filler loading.

3.5. FTIR studies

The FTIR spectrum in Fig. 7 is evidence for interactions between the polymer host and LiFAP salt. Characteristic vibrational bands of PVdF–HFP at 531, 766, and 976 cm^{-1}, corresponding to the α phase crystals are clearly seen. There are, in addition, bands at 484 and 841 cm^{-1} corresponding, respectively, to the β and γ phases [29]. The bands at 839 and 879 cm^{-1} correspond to the amorphous phase of the polymer. The band around 613 cm^{-1} is assigned to –C–F– wagging mode and those around 1197 and 1276 cm^{-1} correspond to asymmetric and symmetrical stretching vibrations of the $-CF_2$ group. Peaks at wave numbers 1185 and 1069 cm^{-1} are assigned to the symmetrical stretching mode of $-CF_3$ and $-CF_2$ groups, respectively, in the pure polymer [30]. That at 1303–1025 cm^{-1} is assigned to –C–F– and $-CF_2$ stretching vibrations of LiFAP. The bands 758 and 709 cm^{-1} are assigned to $-CF_3$ bending and –C–F– wagging modes, respectively, of fluoroalkyl group. The peaks at 810 and 976 cm^{-1} are assigned to P–F bonds and –C–C– bonds, respectively, while those at 496 and 535 cm^{-1} correspond, respectively, to the wagging and bending vibrations of $-CF_2$ groups. Fig. 8 shows the FTIR spectra of CPEs with different filler contents. A comparison of Figs. 7 and 8 suggests complex formation and interactions involving the constituents of the polymer electrolyte. In Fig. 8, the bands at 3010 and 2967 cm^{-1} assigned to CH_3 and CH_2 stretching regions of DEC shifted and drastic reduction in intensity which are obviously observed in all the CPEs. This suggests that the complexation of solvent molecules (EC/DEC) with

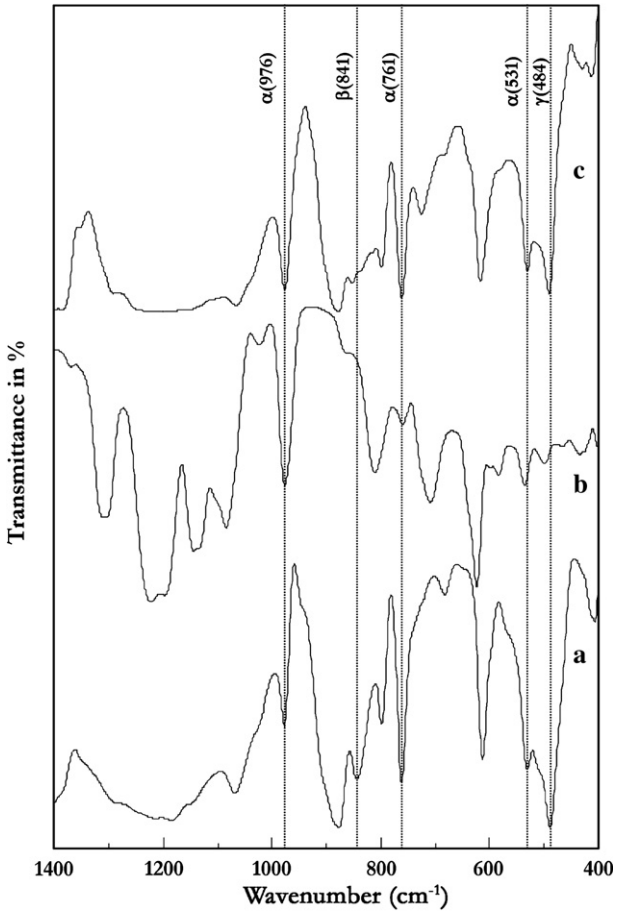

Fig. 7. FTIR spectra of (a) pure PVdF–HFP, (b) pure LiFAP, and (c) PVdF–HFP + LiFAP.

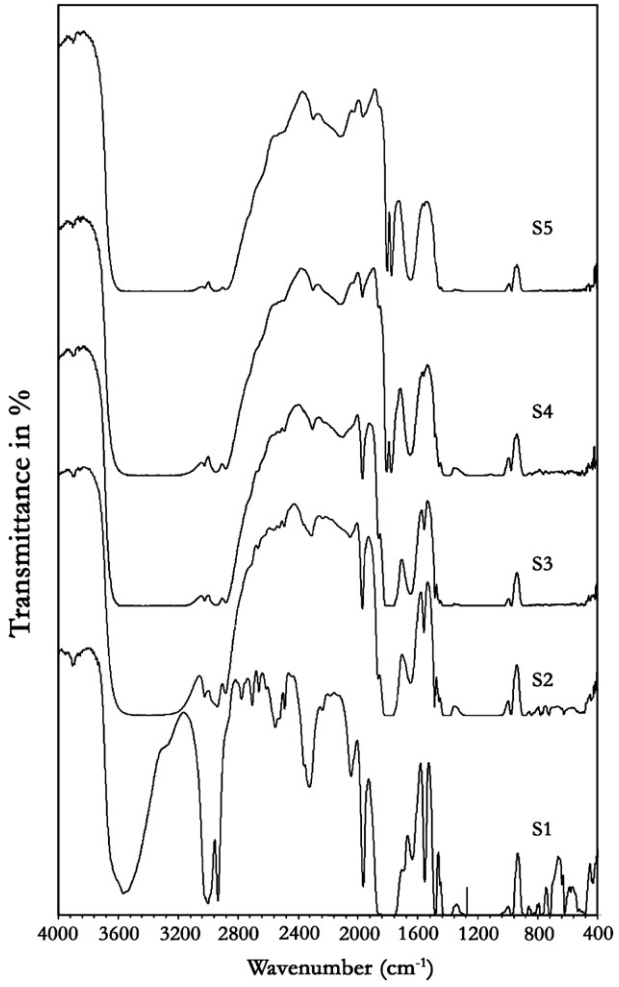

Fig. 8. FTIR spectra of CPEs with different filler contents (wt%): 0.0 (S1), 2.5 (S2), 5.0 (S3), 7.5 (S4), and 10.0 (S5).

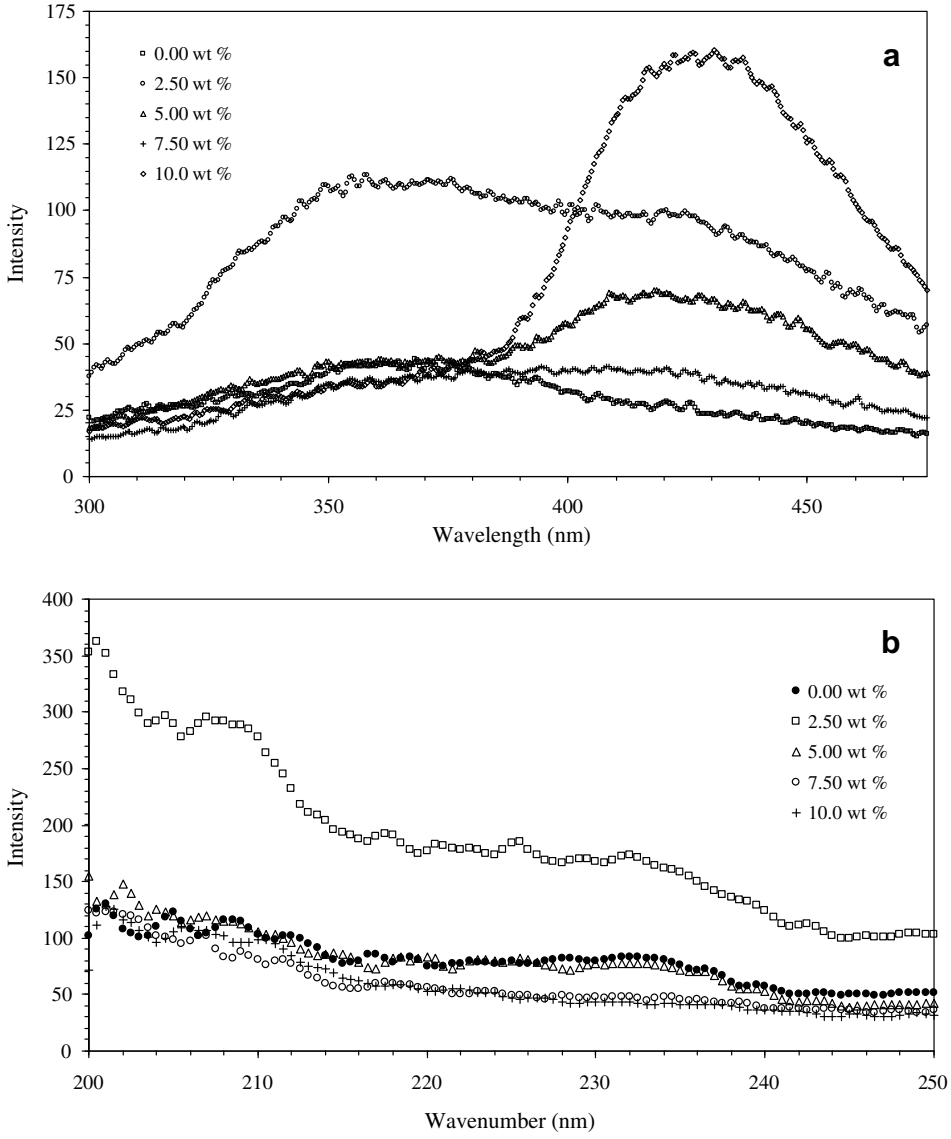

Fig. 9. (a) Photoluminescence emission spectra of CPEs at different filler concentrations, excitation by λ_{exc} = 280 nm; and (b) photoluminescence excitation spectrum of CPEs at different filler concentrations, emission λ_{emn} = 360 nm.

acidic surface group of the nanoscopic Al_2O_3. The CH_2 bending mode of DEC (1479 cm^{-1}) is observed only in filler free and 2.5 wt% CPEs. Ring breathing mode of EC is obviously observed at 976 cm^{-1} in all the electrolytes with decrease in intensity after the loading of Al_2O_3. The bands of DEC at 895 (–OCOO– out of plance deformation), 855 (CH_2 rocking) and 793 cm^{-1} (out of plane skeleton deformation) are diminished after the addition of nanoscopic Al_2O_3 [31]. Similarly, the drastic decrease in CH_2 bending mode (1480 cm^{-1}) of EC is decreased after the addition of 2.5 wt% of Al_2O_3 and it is diminished by further addition of fillers. EC bands at 1865 (C=O stretching), 1394 (CH_2 wagging) and 720 (C=O bending) are observed for filler free and 2.5 wt% membranes only [32]. The diminishing of such intensities is not only due to acidic surface groups of the nanoscopic Al_2O_3 but interaction with $–CF_2$ group of polymer as well the fluoroalkyl group of LiFAP.

3.6. Fluorescence studies

Ionic mobility in porous structures cannot be correlated directly with the macroscopic viscosity measured usually by rheometric methods [33]. In fact, ionic mobility in these structures is related to the local viscosity surrounding the charge carriers. Fluorescence studies provide information on local viscosity effects in polymeric media. This technique can also detect structural alterations in the local environments and has been used to study the structural, conformational and dynamic properties of polymer systems [34]. The intensity values are directly proportional to the local viscosity of the surrounding polymeric media.

Typical fluorescence emission and excitation spectra of CPEs with different filler loadings are given in Fig. 9a and b. It can be seen that the CPE with 2.5 wt% filler concentration shows a higher intensity than the other membranes. This suggests that molecular motion in composite polymer systems is hindered above certain filler concentrations. The higher viscosities of the polymeric medium leads to decrease in mobility of the ions, which translates into reduced conductivity. The enhancement in local viscosity may be attributed to a strong interaction between the filler particles and the polymer host, resulting in sluggish segmental motion of polymer chains.

4. Conclusions

LiFAP-based polymer electrolytes with 2.5 wt% nanoparticulate Al_2O_3 filler exhibits an ambient temperature ionic conductivity of

0.98 m S cm^{-1}. The presence of the filler particles reduces the T_m of the polymeric membrane to lower temperatures (as much as 85 °C at a filler concentration of 2.5 wt%). The lowering of the crystalline nature of the CPE leads to improved conductivity. The filler particles also lead to local viscosity changes in the polymeric matrix, which can be detrimental to ion transport above certain filler concentrations.

Acknowledgments

V.A. is grateful to Professor Nikolai Ignatyev and Dr Winfried Geissler, Ionic Liquids Research Laboratory, Merck KGaA, Darmstadt, Germany, and Anna Maria Bertasa, Solvay Solexis S.p.A., Italy for kindly supplying LiFAP and PVdF–HFP, respectively.

References

[1] K.M. Abraham, M. Alamgir, J. Electrochem. Soc. 137 (1990) 1657.
[2] M. Alamgir, R.D. Moulton, K.M. Abraham, in: K.M. Abraham, M. Salomon (Eds.), Primary and Secondary Lithium Batteries, The Electrochemical Society, Pennington, NJ, 1991, p. 131.
[3] K.M. Abraham, M. Alamgir, J. Power Sources 43&44 (1993) 195.
[4] K.M. Abraham, M. Alamgir, Chem. Mater. 3 (1991) 339.
[5] K.M. Abraham, in: B. Scrosati (Ed.), Applications of Electroactive Polymers, Chapman & Hall, London, 1993 (Chapter 3).
[6] F. Croce, F. Bonino, S. Panero, B. Scrosati, Philos. Mag. B 59 (1989) 161.
[7] G. Wang, G. Pistoia, J. Electroanal. Chem. 302 (1991) 275.
[8] D. Aurbach, Y. Talyosef, B. Markovsky, E. Markevich, E. Zinigrad, L. Asraf, J.S. Gnanaraj, H.J. Kim, Electrochim. Acta 50 (2004) 247.
[9] S.S. Zhang, K. Xu, T.R. Jow, J. Electrochem. Soc. 149 (2002) A586.
[10] S.S. Zhang, K. Xu, T.R. Jow, Solid State Ionics 158 (2003) 375.
[11] K. Kanamura, W. Hoshikawa, T. Umegaki, J. Electrochem. Soc. 149 (2002) 339.
[12] S.E. Sloop, J.K. Pugh, S. Wang, J.B. Kerr, K. Kinoshita, Electrochem. Solid-State Lett. 4 (2001) A42.
[13] E. Zinigrad, L. Larush-Asraf, J.S. Gnanaraj, M. Sprecher, D. Aurbach, Thermochim. Acta 438 (2005) 184.
[14] D. Aurbach, K. Gamolsky, B. Markovsky, G. Salitra, Y. Gofer, J. Electrochem. Soc. 147 (2000) 1322.
[15] Z.B. Zhou, M. Tskeda, M. Ue, Solid State Ionics 177 (2006) 323.
[16] M. Schmidt, U. Heider, A. Kuehner, R. Oesten, M. Jungnitz, N. Ignat'ev, P. Sartori, J. Power Sources 97&98 (2001) 557.
[17] R. Oesten, U. Heider, M. Schmidt, Solid State Ionics 148 (2002) 391.
[18] J.S. Gnanaraj, E. Zinigrad, L. Asraf, M. Sprecher, H.E. Gottlieb, W. Geissler, M. Schimidt, D. Aurbach, Electrochem. Commun. 5 (2003) 946.
[19] J.S. Gnanaraj, M.D. Levi, Y. Gofer, D. Aurbach, M. Schmidt, J. Electrochem. Soc. 150 (2003) A445.
[20] J.S. Gnanaraj, E. Zinigrad, M.D. Levi, D. Aurbach, M. Schmidt, J. Power Sources 119&121 (2003) 799.
[21] E. Zinigrad, L.L. Asraf, J.S. Gnanaraj, H.E. Gottlieb, M. Sprecher, D. Aurbach, J. Power Sources 146 (2005) 176.
[22] V. Aravindan, P. Vickraman, T. Prem Kumar, J. Membr. Sci. 305 (2007) 146.
[23] C.W. Nan, L. Fan, Y. Lin, Q. Cai, Phys. Rev. Lett. 91 (2003) 266104.
[24] H. Wang, H. Huang, S.L. Wunder, J. Electrochem. Soc. 147 (2000) 2853.
[25] H.J. Rhoo, H.T. Kim, J.M. Park, T.S. Hwang, Electrochim. Acta 42 (1997) 1571.
[26] P. Sajkiewicz, Eur. Polym. J. 35 (1999) 1581.
[27] K.M. Kim, N.G. Park, K.S. Ryu, S.H. Chang, Electrochim. Acta 51 (2006) 5636.
[28] J.Y. Song, Y.Y. Wang, C.C. Wan, J. Electrochem. Soc. 147 (2000) 3219.
[29] R. Gregorio Jr, M. Cestari, J. Polym. Sci. B 26 (1994) 859.
[30] Z. Li, G. Su, D. Gao, X. Wang, X. Li, Electrochim. Acta 49 (2004) 4633.
[31] J. Wang, Y. Wu, X. Xuan, H. Wang, Spectrochim. Acta A 58 (2002) 2097.
[32] Z. Osman, A.K. Arof, Electrochim. Acta 48 (2003) 993.
[33] U.S. Park, Y.J. Hong, S.M. Oh, Electrochem. Acta 41 (1993) 849.
[34] D.A. Waldow, M.D. Ediger, T. Tamaguchi, T. Matsushita, E. Noda, Macromolecules 24 (1991) 3147.